NIH Public Access
Author Manuscript
Dev Biol. Author manuscript; available in PMC 2013 December 04.

Published in final edited form as:
Dev Biol. 2012 August 15; 368(2): . doi:10.1016/j.ydbio.2012.05.037.

A cell-autonomous defect in skeletal muscle satellite cells expressing low levels of survival of motor neuron protein

Monica Hayhurst[a], **Amanda K. Wagner**[a], **Massimiliano Cerletti**[a], **Amy J. Wagers**[a,b,c], and **Lee L. Rubin**[a,b,*]

[a]Department of Stem Cell and Regenerative Biology, USA

[b]Harvard Stem Cell Institute, Harvard University, Sherman Fairchild Bldg, 7 Divinity Avenue, Cambridge, MA 02138, USA

[c]Howard Hughes Medical Institute, USA

Abstract

Mutations in the Survival of Motor Neuron (SMN) gene underlie the development of spinal muscular atrophy (SMA), which currently represents the leading genetic cause of mortality in infants and toddlers. SMA is characterized by degeneration of spinal cord motor neurons and muscle atrophy. Although SMA is often considered to be a motor neuron disease, accumulating evidence suggests that muscle cells themselves may be affected by low levels of SMN. Here, we examine satellite cells, tissue-resident stem cells that play an essential role in the growth and repair of skeletal muscle, isolated from a severe SMA mouse model ($Smn^{-/-}$; $SMN2^{+/+}$). We found similar numbers of satellite cells in the muscles of SMA and wild-type ($Smn^{+/+}$; $SMN2^{+/+}$) mice at postnatal day 2 (P2), and, when isolated from skeletal muscle using cell surface marker expression, these cells showed comparable survival and proliferative potential. However, SMA satellite cells differentiate abnormally, revealed by the premature expression of muscle differentiation markers, and, especially, by a reduced efficiency in forming myotubes. These phenotypes suggest a critical role of SMN protein in the intrinsic regulation of muscle differentiation and suggest that abnormal muscle development contributes to the manifestation of SMA symptoms.

Keywords

Spinal muscular atrophy; Satellite cells; Muscle

Introduction

Spinal muscular atrophy (SMA) is an autosomal recessive disease and a leading cause of infant mortality (Park et al., 2010). SMA is characterized by proximal skeletal muscle weakness, stemming at least in part from the degeneration of anterior horn cells of the spinal cord (Crawford and Pardo, 1996). The underlying cause of human SMA is mutation of the *SMN1* gene, which results in diminished levels of full length SMN (DiDonato et al., 1997; Lefebvre et al., 1995; Lorson et al., 1999). SMA patients have dramatically reduced levels of the SMN protein, and disease severity inversely correlates with the amount of full-length protein expressed (Coovert et al., 1997; Feldkotter et al., 2002; Gavrilov et al., 1998). The

© 2012 Elsevier Inc. All rights reserved

*Correspondence at: Harvard University, Dept. of Stem Cell and Regenerative Biology, Sherman Fairchild Bldg, 7 Divinity Avenue, Cambridge, MA 02138, USA. Fax: +1617 495 3961. lee_rubin@harvard.edu (L.L. Rubin).

NIH-PA Author Manuscript
NIH-PA Author Manuscript
NIH-PA Author Manuscript

NIH-PA Author Manuscript

NIH-PA Author Manuscript

NIH-PA Author Manuscript

most severe form of SMA manifests during the course of motor unit development and causes profound muscle weakness (Crawford and Pardo, 1996).

In vivo models have consistently demonstrated a critical role of SMN in motor neurons. Morpholino-mediated knockdown of *Smn* in zebrafish severely truncates axonal extension and disturbs pathfinding of motor neurons (McWhorter et al., 2003). Isolated motor neurons from $Smn^{-/-}$;$SMN2^{+/+}$ mice show abnormalities in axonal growth and growth cone morphology, but exhibit normal survival (Rossoll et al., 2003). In another severe SMA mouse model ($Smn^{-/-}$;$SMN2^{+/+}$;$SMN\Delta7^{+/+}$), which typically exhibits mortality approximately two weeks after birth, a similar denervation phenotype as well as abnormal synaptic transmission was observed (Le et al., 2005).

Muscle atrophy is also a widely accepted hallmark of SMA, and a growing body of evidence suggests that muscle pathology could have an important primary role in this disease. In both mice and flies, high levels of Smn are reported to localize to the myofiber, suggesting a muscle-specific function (Chang et al., 2008; Rajendra et al., 2007). Additional evidence suggests that high levels of SMN are critical for the survival of myogenic (muscle-forming) cells. For example, cultured myogenic cells harboring a deletion of SMN exon 7, thus producing a rapidly degrading truncated form of the protein, showed increased cell death through a non-apoptotic process (Nicole et al., 2003). Furthermore, knockdown of *Smn* in C2C12 myoblasts reduces their proliferation in a dose dependent manner, such that cells with the most reduced Smn protein levels exhibit the most dramatic reduction in growth potential (Shafey et al., 2005). Studies conducted in mouse models strongly suggested an additional role for SMN in muscle development and maintenance. In the most severe SMA model, muscle fibers are reduced in size in late symptomatic (P5-P6) mice, with slow-twitch postural muscles more affected than fast-twitch phasic muscles (Monani et al., 2000; Murray et al., 2008). Selectively abolishing Smn expression in muscle tissue results in a prominent dystrophic phenotype, characterized by myofiber necrosis associated with destabilization of sarcolemma components (Cifuentes-Diaz et al., 2001). Interestingly, this phenotype could be improved by maintaining Smn expression in myogenic precursors, with depletion of Smn only in multinucleated myotubes, (Nicole et al., 2003). Moreover, SMN-deficient myotubes cultured from SMA patient biopsies are small in size compared to myotubes prepared from normal patient biopsy tissue (Guettier-Sigrist et al., 2002). Additionally, co-cultures of muscle from severe SMA patients with wild-type motor neurons exhibit considerable muscle degeneration, as well as motor neuron apoptosis. In contrast, muscles from control or patients with type III SMA, the least severe form of SMA (Campbell et al., 1997; Feldkotter et al., 2002; Lefebvre et al., 1995), maintained stable connections, indicating a muscle specific requirement for SMN (Braun et al., 1995; Guettier-Sigrist et al., 2002; Henderson et al., 1987).

Thus, a great deal of work points to an independent role for Smn in muscle development and function. This was further suggested by a recent study in which another SMA mouse model ($Smn^{-/-}$;$SMN2^{+/+}$;$SMN\Delta7^{+/+}$) was seen to exhibit muscle weakness correlated with smaller fiber number and smaller fiber size. The delay in muscle development appeared during a period of rapid postnatal muscle growth and in the absence of motor neuron loss (Lee et al., 2011).

Because much of muscle growth in that period is driven by the proliferation and differentiation of muscle satellite cells, we focused on the behavior of these cells in neonatal mice ($Smn^{-/-}$;$SMN2^{+/+}$) that model the most severe form of SMA. Satellite cells, located between the sarcolemma and the basal lamina of muscle fibers, are muscle stem cells and represent the major regenerative population in skeletal muscle. The satellite cell population, denoted by the expression of Pax7 in the absence of committed myogenic lineage markers

NIH-PA Author Manuscript

NIH-PA Author Manuscript

NIH-PA Author Manuscript

such as MyoD, is responsible for most early neonatal muscle growth and is required for maintenance and repair of adult muscle, as also has been demonstrated by transplantation studies using purified satellite cell populations (Blanco-Bose et al., 2001; Cerletti et al., 2008; Collins et al., 2005; Cornelison et al., 2001; Kuang et al., 2007; Montarras et al., 2005).

Here we show that P2 SMA mouse hindlimb muscles are smaller in this mouse model, as they were in the one used by Lee et al. (2011). This is due to a combination of reduced myofiber number and average size. We further demonstrate that the reduction in size is accompanied by the accumulation of satellite cells that have undergone premature differentiation. We isolated satellite cells from neonatal muscle and show that, when maintained in cell culture, they too begin to differentiate more rapidly than cells isolated from control muscle. Most significantly, however, these cells fail to form multinucleated myotubes efficiently. These data indicate that SMN plays a critical role in myogenesis, with adequate SMN required for normal differentiation. These results further demonstrate the existence of a cell autonomous defect in Smn-deficient muscle satellite cells that is manifest in the absence of motor neurons. In light of these findings, we suggest that the most effective SMA therapeutics will be directed at both muscle satellite cells and motor neurons.

Experimental procedures

Mice

Smn$^{-/-}$;*SMN2*$^{+/+}$ mice (FVB.Cg–Tg(SMN2)89Ahmb *Smn1*$^{tm1\ Msd}$/J Jackson Laboratories, Bar Harbor, ME, USA) were maintained as heterozygotes for *Smn* (Monani et al., 2000). Genotyping was done by polymerase chain reaction (PCR), as described on the Jackson Laboratories website. All experiments were performed on P0 or P2 *Smn*$^{-/-}$;*SMN2*$^{+/+}$ (SMA mice) or *Smn*$^{+/+}$;*SMN2*$^{+/+}$ (control) litter-mates. Mice were maintained at the Harvard University animal facility according to institutionally approved protocols.

Satellite cell isolation

Myofiber-associated cells were prepared from intact limb muscle as described (Cerletti et al., 2008; Conboy et al., 2003; Sherwood et al., 2004) with the following modifications. Muscle tissue was digested in Dulbecco's modified Eagle's medium (Invitrogen, Carlsbad, CA) with 0.2% (w/v) collagenase II (Invitro-gen, Carlsbad, CA) for 20 min at 37 °C. Tissue was dissociated into single myofibers by repeated trituration with a Pasteur pipette in phosphate buffered saline (PBS). A second digestion with 0.0125% collagenase I and 0.05% dispase (Invitrogen, Carlsbad, CA) was performed for 30 min at 37 °C. Antibody staining of satellite cells was carried out as described previously (Cerletti et al., 2008; Sherwood et al., 2004). Flow cytometry analysis and cell sorting were performed on a Mo-Flo cell sorter (Beckman Colter, Brea, CA) or BD FACSAria II (BD Biosciences, San Jose, CA). Cells that were CD45^{-},Sca-1^{-},Mac-1^{-},CXCR4^{+},β1-integrin^{+} were isolated by double-sorting, to ensure purity (Cerletti et al., 2008; Sherwood et al., 2004). We typically obtained approximately 80,000–100,000 satellite cells per P2 animal.

Cell culture

For growth conditions (clonal assay and high density proliferation), four hours prior to adding cells, plates were coated with 10 μg/ml laminin (Invitrogen, Carlsbad, CA) and 1 μg/ml collagen (Sigma-Aldrich, St. Louis, MO). For clonal assays, cells were double-sorted, and plated as single cells in 96-well tissue culture plates. For bulk cultures, 5×10^3 cells were plated per well in 48-well plates or 5×10^2 cells were plated per well in 96-well plates. Growth medium (GM) was composed of Ham's F10, 20% horse serum, 1% penicillin/streptomycin, 1% glutamine, and 5 ng/ml bFGF (Invitrogen, Carlsbad, CA). Cells were

NIH-PA Author Manuscript

NIH-PA Author Manuscript

NIH-PA Author Manuscript

cultured for four days in GM, with fresh bFGF supplemented each day. For myotube formation assays, four hours prior to plating, plates were coated with 10 μg/ml laminin. 5×10^2 cells were plated, grown in GM supplemented with bFGF for 4 days and then switched to differentiation medium (DM), composed of DMEM, 10% horse serum, 10% fetal bovine serum, 1% glutamine, 1% sodium pyruvate, 50 ng/ml Gentamycin and 0.5% chick embryo extract and maintained in these conditions for the duration of the experiment.

Immunoblot analysis

Cells were lysed with RIPA buffer (Thermo Fisher Scientific, Waltham, MA) supplemented by addition of complete protease and phosphatase inhibitor cocktails (VWR Radnor, PA). Cell lysates were resolved by electrophoresis through a 10% Tris-Glycine Novex gel and transferred to PVDF membranes (Invitrogen, Carlsbad, CA) using a semi-dry transfer apparatus. Membranes were incubated overnight with a 1:10,000 dilution of monoclonal anti-SMN antibody (MAB8, BD Biosciences, San Jose, CA) and 1 h with monoclonal anti-human β-tubulin antibody diluted 1:10,000 (Abeam, Cambridge, MA). Primary antibodies were detected by enhanced chemi-luminescence (West Pico Reagent, Pierce, Rockford, IL, USA) using secondary antibodies conjugated with horseradish peroxidase (goat anti-mouse for SMN and goat anti-rabbit for β-tubulin; Thermo Fisher, Waltham, MA).

Immunostaining

Whole hindlimbs were fixed (4% paraformaldehyde, 1 h), paraffin embedded and sectioned at 4.5 μm. Sections were incubated with xylene to remove paraffin and rehydrated through a series of 100%, 95%, 70%, 50% ethanol washes. Antigen retrieval was performed at 95 °C for 30 min in 10 mM sodium citrate buffer, 0.05% Tween 20, pH 6.0, blocked with 10% goat serum in PBS, and sections were immunostained with a rabbit anti-dystro-phin antibody (1:400; Abcam, Cambridge, MA). Sections were washed in PBS and then incubated in goat anti-rabbit Alexa 488 (1:1000; Invitrogen, Carlsbad, CA). Finally, sections were washed with PBS and mounted with VECTASHIELD Mounting Medium with DAPI (Vector Laboratories, Burlingame, CA). Measurements of the number and size of fibers were taken on comparable sections.

Frozen muscle sections embedded in optimum cutting temperature compound (OCT) from fixed, (4% paraformaldehyde, 1 h) whole hindlimbs were sectioned at 8 μm. Sections were fixed again (4% paraformaldehyde, 10 min), and antigen retrieval was performed at 95 °C for 10 min in 10 mM sodium citrate buffer, 0.05% Tween 20 pH 6.0. Sections were blocked with 10% goat serum and immunostained with a rabbit anti-MyoD antibody (1:400; Santa Cruz Biotechnology, Santa Cruz, CA) and an anti-Pax7 antibody (1:25; Developmental Studies Hybridoma Bank, Iowa City, IA). Sections were washed in PBS and then incubated in goat anti-rabbit Alexa 488 (1:1000; Invitrogen, Carlsbad, CA) and anti-mouse Alexa 546 (1:1000; Invitrogen, Carlsbad, CA) for 1 h. Finally, sections were washed with PBS and mounted with VECTASHIELD Mounting Medium with DAPI. $Pax7^+$ and $MyoD^+$ cells were identified in comparable sections of the tibialis anterior (TA), extensor digitorum longus (EDL), and soleus muscles. The number of $Pax7^+/MyoD^-$ or $Pax7^+/MyoD^+$ cells was normalized to the number of fibers.

For some studies, immunostaining was carried out on cells that were allowed to adhere to a Superfrost Plus glass slide. Cells were fixed (4% paraformaldehyde, 10 min), permeabilized with 0.2% Triton X-100/PBS, blocked with 50:50 MOM Blocking (Vector Laboratories, Burlingame, CA) and 10% horse serum in PBS, and stained with chicken anti-syndecan-4 (1:400; Olwin laboratory, University of Colorado Boulder), mouse anti-Pax7 antibody (1:25; Developmental Studies Hybridoma Bank, Iowa City, IA), rabbit anti-MyoD antibody (1:200; Santa Cruz Biotechnology, Santa Cruz, CA) or rabbit anti-myogenin (1:400; Santa

NIH-PA Author Manuscript

NIH-PA Author Manuscript

NIH-PA Author Manuscript

Cruz Biotechnology, Santa Cruz, CA). Cells were washed with PBS and then stained with goat anti-chicken Alexa 594, goat anti-rabbit Alexa 594 or goat anti-mouse Alexa 488 (1:1000; Invitrogen, Carlsbad, CA). Nuclei were stained with Hoechst or DAPI (1:5000).

For the analysis of myotube formation, cultures were fixed with 4% paraformaldehyde for 10 min, permeabilized with 0.2% Triton X-100/PBS, blocked with 5% goat serum in PBS, and stained with a mouse anti-fast skeletal muscle myosin antibody (1:400; Sigma-Aldrich, St. Louis, MO). Cells were washed with PBS and then stained with goat anti-mouse Alexa 488 (1:1000; Invitrogen, Carlsbad, CA). Nuclei were stained with Hoechst. For some experiments, we determined the incidence of cell death using a TUNEL labeling kit (Roche, Indianapolis, IN).

Microscopy

Fluorescence and brightfield images were acquired using a standard Olympus BX60 microscope or Nikon Eclipse TE 2000-S microscope. Fluorescence images were acquired using DP Manager (Olympus Optical CO, LTD) or NIS Elements BR3.0. Fiber area was determined by quantifying 100 fibers per muscle and determining the area using NIS Elements BR3.0 software.

Results

Neonatal SMA type I animals have normal numbers of satellite cells

In these studies, we focused on skeletal muscle development using a severe SMA mouse model ($Smn^{-/-}$;$SMN2^{+/+}$). Newborn SMA mice were indistinguishable from control littermates, but rapidly developed a clear pathology characterized by an inability to suckle, reduced size, and progressive weakness after P2 (Monani et al., 2000). SMA mice at P3 were noticeably smaller than their wildtype counterparts. Staining was carried out on transverse paraffin sections of the TA, EDL, and soleus muscles using an anti-dystrophin antibody to outline individual fibers (Fig. 1A). At PO, muscle fiber numbers appeared normal. Between PO and P2, the number of muscle fibers in control muscle, but not in SMA muscle, increased slightly. The end result was that there was a small, but statistically significant, difference in the number of fibers between control and SMA muscles at P2 (Fig. 1B). In addition, fibers from all three SMA muscles examined at P2 also had smaller cross sectional areas (Fig. 1C,D). Thus, even at an early time, when SMA pups appear grossly normal, they exhibited a clear reduction in the total number of muscle fibers and in fiber area in all muscles sampled.

The fact that the number of fibers in SMA muscle did not appear to *decrease* dramatically between days PO and P2 argues against muscle degeneration accounting for the differences in size at the later time point. The other possibility is that the rates of muscle growth in the two genotypes of mice are different. Muscle satellite cells, which reside outside of multinucleated muscle cells, give rise to myogenic precursors that participate in the *de novo* generation of fibers and addition of nuclei to existing fibers (Hawke and Garry, 2001; Wagers and Conboy, 2005; Zammit, 2008). The process of muscle development involves two populations of Pax7-expressing cells: self-renewing satellite cells ($Pax7^{+}/MyoD^{-}$) and more differentiated muscle progenitors ($Pax7^{+}/MyoD^{+}$) (Supplementary Fig. 1). A fraction of $Pax7^{+}/MyoD^{+}$ cells are able to return to quiescence and re-enter the satellite cell pool (Seale et al., 2000; Zammit, 2008) (Supplementary Fig. 1). Thus, we measured various properties of the satellite cell and muscle progenitor pools at P2.

Transverse sections of lower hindlimb muscles were stained with anti-Pax7 and anti-MyoD antibodies to discriminate between satellite cells and more differentiated myogenic cells

NIH-PA Author Manuscript

NIH-PA Author Manuscript

NIH-PA Author Manuscript

(Fig. 2A). Curiously, we observed an apparent increase in the numbers of nuclei *per fiber* that were only $Pax7^+$ in SMA muscle, with some muscles, such as the EDL, having a larger difference than others (Fig. 2B). Even though SMA muscles have fewer fibers, the total number of satellite cells per muscle appears to be roughly equivalent to the number in control muscles. Interestingly, we also observed a higher number of Pax7 and MyoD co-positive cells per fiber in transverse sections of SMA muscle (Fig. 2C) so that a significantly higher percentage of $Pax7^+$ nuclei also expressed MyoD (Fig. 2D). The enrichment of myogenic progenitors in SMA muscles suggested enhanced production of a more differentiated myogenic cell type.

To study further potential perturbations in satellite cell proliferation and differentiation in SMA mice, we used fluorescence activated cell sorting (FACS) to isolate these cells. $CD45^-Sca\text{-}1^-Mac\text{-}1^-CXCR4^+\beta1\text{-}integrin^+$ cells are self-renewing muscle stem cells that, under appropriate conditions, efficiently form myogenic colonies in vitro and generate multinucleated myofi-bers when maintained in vitro or transplanted in vivo (Cerletti et al., 2008; Sherwood et al., 2004). Previous work has demonstrated that > 90% of FACS purified cells isolated from adult skeletal muscle express Pax7 (Cerletti et al., 2008). Consistent with those studies, Pax7 immunostaining of satellite cells sorted from the skeletal muscle of either neonatal control or SMA mice (Fig. 3A) showed that the vast majority of these cells express Pax7 (Fig. 3B). Furthermore, all freshly sorted cells were positive for the satellite cell marker Syndecan-4 (Fig. 3C) (Cornelison et al., 2001) and negative for MyoD, although, as anticipated, they began to express MyoD after a few days in culture (Fig. 3D). Thus, this protocol produced a highly enriched population of satellite cells from P2 SMA and control muscles.

The number of cells in mutant and control P2 muscle was quantified by FACS (Fig. 4A,B). Muscle interstitial cells, which include fibroblasts and adipogenic precursor cells, marked by expression of Sca-1, (Joe et al., 2010; Schulz et al., 2011; Uezumi et al., 2010) and infiltrating hematopoietic cells ($CD45^+/Mac\text{-}1^+$), were present at comparable frequencies (Fig. 4A,B). The average total number of satellite cells harvested per animal from P2 SMA and control mice was also comparable, although there appeared to be a tendency towards a smaller number in SMA muscle ($8.4 \pm 4.2 \times 10^4$ per set of hindlimb muscles) as compared to wild-type muscle ($1.1 \pm 4.3 \times 10^5$ per set of hindlimb muscles). Together, these data are consistent with our immunocytochemical analysis of muscle tissue in situ and suggest that the reduction of muscle fibers observed in SMA muscles occurs without marked decreases in satellite cell number.

Satellite cells from SMA mice have normal survival and proliferation capacity

Because SMA muscles have smaller and/or fewer fibers, but an approximately normal number of satellite cells, we next investigated whether the function of the satellite cells might be defective in some other way, as was suggested by our observation of an abnormally large number of $Pax7^+/MyoD^+$ cells in SMA muscle. We first assessed their proliferative and survival capacities, as reduction of Smn has been reported to impair survival and proliferation in cultured C2C12 myoblasts (Shafey et al., 2005). To examine myogenic colony forming capacity, we isolated individual satellite cells from P2 control and Smn deficient muscles and cultured these cells clonally for four days under high serum conditions that promote proliferation (Sherwood et al., 2004). On the fourth day in vitro (DIV4), each well was examined for the presence of myogenic cells to determine if reduced levels of Smn resulted in diminished establishment or expansion of myogenic colonies. The frequency of colony formation was approximately 30% for both SMA and control satellite cells (Fig. 5A). The average size (cells per colony) of colonies was also equivalent between the two genotypes (Fig. 5B), as was the distribution of clone size (Fig. 5C). Thus, sorted

NIH-PA Author Manuscript

NIH-PA Author Manuscript

NIH-PA Author Manuscript

satellite cells from mutant and wild-type mice exhibit similar survival and proliferative capacity under optimal growth conditions in vitro.

SMA satellite cells undergo premature differentiation in vitro

As SMA satellite cells displayed no significant differences in proliferation or survival, we next considered whether aberrant differentiation of the satellite cell population might underlie defective development of SMA muscle. This possibility was strongly suggested by our finding that a significantly higher percentage of SMA Pax7$^+$ cells in vivo expressed the myogenic marker MyoD. First, we confirmed that SMA muscle satellite cells seeded at high density in growth-promoting conditions maintained very low levels of SMN (Supplementary Fig. 2A,B). When both types of satellite cells were newly plated, they were mostly small and round, with very few elongated cells. However, by DIV4, mutant cultures contained a higher frequency of cells with a larger cytoplasmic volume and bipolar morphology more closely resembling differentiated myoblasts (Fig. 6A,B). To characterize these cultures further, we first stained them with the Pax7 antibody (Zammit, 2008). SMA and control cultures showed similar percentages of Pax7$^+$ cells when assessed at two different time points (DIV2 or DIV4; Fig. 6C).

This left the possibility that the Pax7$^+$ cells grown in vitro might behave like their in vivo counterparts and accelerate their expression of muscle precursor markers. Thus, we examined DIV2 and DIV4 cultures for MyoD expression. At DIV2, approximately 40% of cells from both SMA and control cultures expressed MyoD (Fig. 7A,B). Over the next two days in culture, the percentage of cells expressing MyoD increased for cells of both genotypes, as expected, but the increase was twice as rapid for the Smn deficient cells (Fig. 7A,B). Because the percentage of Pax7$^+$ cells was identical in the two types of cultures, we predicted that some of the MyoD$^+$ cells in these cultures would co-express Pax7, representing a pool of myogenic progenitors. Cells from DIV4 cultures were co-stained for MyoD and Pax7 to determine the frequency of Pax7$^+$/MyoD$^-$ cells, Pax7$^+$/MyoD$^+$ cells, and Pax7$^-$/MyoD$^+$ cells. We found that SMA cultures contained fewer Pax7$^+$/MyoD$^-$ stem cells ($p < 0.05$), but had a higher frequency of Pax7$^+$/MyoD$^+$ cells that are presumptive myogenic progenitors. About 65% of the wildtype Pax7$^+$ cells were also MyoD$^+$, whereas that percentage increased to almost 90% for the Smn-deficient Pax7$^+$ cells. The frequency of Pax7$^-$/MyoD$^+$ cells was comparable (Fig. 7C,D). We also examined the expression of myogenin, another gene important in myoblast differentiation (Supplementary Fig. 1) (Venuti et al., 1995). At DIV2, SMA cultures have more myogenin positive cells than wild-type culture, though this is not statistically significant (Fig. 7E,F). However, at DIV4 the percentage of myogenin positive cells in SMA cultures is almost twice that of wild-type cultures (Fig. 7E,F). These data indicate that Smn deficient satellite cells transition to a more differentiated population more quickly than control satellite cells, again consistent with what we observed occurring in vivo.

SNA satellite cells make fewer multinucleated myotubes

When myogenic progenitors differentiate into myoblasts, Pax7 expression is extinguished. Myoblasts express MyoD and then myogenin as they become terminally differentiated, finally fusing to form multinucleated myotubes that express myosin heavy chain (MyHC) (Supplementary Fig. 1). To determine if the prematurely differentiating Smn deficient myogenic cells showed defects in myotube formation, we plated satellite cells at high density under high serum conditions to promote proliferation for several days, and then induced myotube formation by switching the cells to a differentiation medium. The number of multinucleated cells that stained with an antibody to myosin heavy chain (MyHC) was measured (Fig. 8A). No MyHC expressing cells were observed after only one day in differentiation medium, and after two days SMA and wild-type cultures contained the same

NIH-PA Author Manuscript

NIH-PA Author Manuscript

NIH-PA Author Manuscript

number of newly formed small myotubes (Fig. 8A,B). However, after 3 days in differentiation medium, Smn deficient cultures contained fewer MyHC positive cells than did equivalent cultures of control cells (Fig. 8A – C). This is also reflected in their obviously reduced formation of myotubes (Fig. 8D). Thus, it appears SMA myogenic cells express markers of differentiation at relatively higher frequency earlier in the differentiation process, but fail to efficiently undergo the final stage of differentiation.

To address the basis for the reduction in the number of myotubes formed by differentiating SMN deficient satellite cells, we performed TUNEL staining 1–3 days after treatment with differentiation medium to identify apoptotic cells in these cultures; however, TUNEL staining revealed very few apoptotic cells (1–5 TUNEL positive cells per culture originally seeded with 5×10^2 satellite cells) at any of these time points (Supplementary Fig. 3). Therefore, reduced myotube formation observed in Smn deficient cultures is not due to excessive apoptosis. Taken together, these data suggest that satellite cells from Smn deficient muscle show a clear defect in their ability to form myotubes, even when cultured under conditions promoting myogenic differentiation. This cell-intrinsic differentiation defect may underlie the reduced myofiber number and size in P2 SMA mice.

Discussion

The most well described and studied characteristic of SMA is motor neuron degeneration; therefore, muscle weakness in this disease has been attributed primarily to neuronal dysfunction (Cifuentes-Diaz et al., 2002; Kariya et al., 2008; McGovern et al., 2008; Murray et al., 2008). Although this is likely to contribute significantly to muscle atrophy as the disease progresses, it does not preclude the possibility that reduced SMN levels in muscle lineage cells, which normally express SMN protein throughout myogenic differentiation and development, may contribute independently to the SMA phenotype. Consistent with this notion, and with the findings of Lee et al. (2011) using a different mouse SMA model, we found limb muscles of SMA mice contained significantly fewer and smaller myofibers at P2 than their wild-type counterparts.

Since satellite cells are responsible for the bulk of muscle growth in the early postnatal period, we examined their behavior in the SMA mice. We did not observe a dramatic depletion of the satellite cell pool in P2 SMA mice. Staining muscle tissue for Pax7 and MyoD revealed an increased number of satellite cells per fiber, even though the number of fibers was lessened. When FACS purifying satellite cells from whole hindlimb muscle, we isolated roughly comparable total numbers of satellite cells from mutant and control animals. Taken together, these results make it seem unlikely that a depletion of satellite cells causes reduced muscle size. However, it is distinctly possible that satellite cells are depleted at later time points in the course of the disease. To determine if this is the case, it will be necessary to use less severe SMA mice that survive for longer times.

On the other hand, we did observe that a higher frequency of $Pax7^+$ cells in the muscle of SMA mice co-expressed MyoD, strongly suggesting that abnormal differentiation of satellite cells might contribute to faulty muscle development. To test this possibility, we isolated satellite cells using a FACS protocol identical to that used to isolate these cells from wild-type mice, to determine if reduced levels of Smn caused any cell autonomous defect in myogenic cells. Satellite cells from Smn deficient mice formed clonal myogenic colonies with frequencies equal to those of control cells. Furthermore, Smn deficient clones were similar in size to controls, demonstrating that Smn deficient satellite cells and their progeny proliferate normally despite having dramatically reduced levels of Smn, at least over the time course of these experiments. These data suggest that low levels of Smn are still sufficient for muscle satellite cell survival and growth during early neonatal time points.

NIH-PA Author Manuscript

NIH-PA Author Manuscript

NIH-PA Author Manuscript

Nonetheless, SMA satellite cells did also exhibit an aberrant phenotype when maintained in vitro. A higher percentage of these cells became myogenic progenitors, marked by Pax7 and MyoD co-expression, at the expense of Pax7 single-positive muscle stem cells. Smn deficient satellite cells also expressed other myogenic differentiation markers, such as myogenin, and formed MyHC positive cells more quickly than did control satellite cells, further supporting a premature differentiation phenotype in these cells. This finding contrasts with observations made in neural stem cells, where Smn deficient cells show significantly delayed differentiation (Shafey et al., 2008). Most importantly, however, the myogenic cells with low Smn levels displayed a markedly reduced ability to generate multinucleated myotubes in vitro. Cells in the SMA muscle cultures did not appear to undergo increased apoptosis at the time points examined, and further studies will be required to determine their fate. The relative inability of Smn deficient myoblasts to form multinucleated myotubes may explain the muscle defects observed in mice with low levels of Smn.

Experiments presented in this paper were conducted at P0–P2, a time at which Smn deficient animals exhibit few of the more overt changes of SMA (Monani et al., 2000; Murray et al., 2008). Due to the poor viability of older $Smn^{-/-}$;$SMN2^{+/+}$ mice, which can die as early as P3–P4, we chose to analyze animals at earlier time points. Between P0 and P2, SMA mice continue to increase fiber numbers in all muscle groups examined (Fig. 1B), minimizing the possibility that our observations are a consequence of rapid degeneration of the muscle fibers. Our data thus support a cell-autonomous role for SMN protein in postnatal satellite cell function, and it will also be interesting to determine if faulty muscle development can exacerbate the motor neuron defects seen in SMA.

From both in vivo and in vitro work, it is clear that motor neurons are relatively vulnerable to low levels of SMN. However, the data presented here indicates that these defects are unlikely to be the sole cause of the disease pathology. SMN appears to play a critical role in myofiber maturation, which may contribute to the muscle atrophy and resulting weakness that is observed in SMA mouse models and SMA patients. Although elevating expression of SMN in muscle alone fails to alleviate the SMA phenotype in mice (Gavrilina et al., 2008), the work presented here suggests that future therapeutics should be more broadly focused, not only to increase SMN in motor neurons, but also potentially in muscle cells in order to attain the greatest clinical improvement.

Supplementary Material

Refer to Web version on PubMed Central for supplementary material.

Acknowledgments

The authors would like to thank Patrick Heiser, Karen Kotkow and Kelly Haston for helpful comments and Jane Lalonde for editorial assistance. Additionally, we would like to thank Wesley Thompson (University of Texas) for sharing unpublished data, Johanna Lee for assistance with Pax7 antibody staining, and the Joslin Diabetes Center HSCI/DERC funded Flow Cytometry Core (NIH P30 DK036836) for excellent cell sorting. The work was supported by Grants from the Spinal Muscular Atrophy Foundation, NINDS (P01NS066888-01A1) and by the Harvard Stem Cell Institute to LLR, and by awards from the Beckman Foundation and Howard Hughes Medical Institute to AJW.

Appendix A. Supporting information

Supplementary data associated with this article can be found in the online version at http://dx.doi.Org/10.1016/j.ydbio.2012.05.037.

NIH-PA Author Manuscript

NIH-PA Author Manuscript

NIH-PA Author Manuscript

References

Blanco-Bose WE, Yao CC, Kramer RH, Blau HM. Purification of mouse primary myoblasts based on alpha 7 integrin expression. Exp. Cell Res. 2001; 265:212–220. [PubMed: 11302686]

Braun S, Croizat B, Lagrange MC, Warter JM, Poindron P. Constitutive muscular abnormalities in culture in spinal muscular atrophy. Lancet. 1995; 345:694–695. [PubMed: 7741893]

Campbell L, Potter A, Ignatius J, Dubowitz V, Davies K. Genomic variation and gene conversion in spinal muscular atrophy: implications for disease process and clinical phenotype. Am. J. Hum Genet. 1997; 61:40–50. [PubMed: 9245983]

Cerletti M, Jurga S, Witczak CA, Hirshman MF, Shadrach JL, Goodyear LJ, Wagers AJ. Highly efficient, functional engraftment of skeletal muscle stem cells in dystrophic muscles. Cell. 2008; 134:37–47. [PubMed: 18614009]

Chang HC, Dimlich DN, Yokokura T, Mukherjee A, Kankel MW, Sen A, Sridhar V, Fulga TA, Hart AC, Van Vactor D, et al. Modeling spinal muscular atrophy in Drosophila. PLoS One. 2008; 3:e3209. [PubMed: 18791638]

Cifuentes-Diaz C, Frugier T, Tiziano FD, Lacene E, Roblot N, Joshi V, Moreau MH, Melki J. Deletion of murine SMN exon 7 directed to skeletal muscle leads to severe muscular dystrophy. J. Cell Biol. 2001; 152:1107–1114. [PubMed: 11238465]

Cifuentes-Diaz C, Nicole S, Velasco ME, Borra-Cebrian C, Panozzo C, Frugier T, Millet G, Roblot N, Joshi V, Melki J. Neurofilament accumulation at the motor endplate and lack of axonal sprouting in a spinal muscular atrophy mouse model. Hum. Mol. Genet. 2002; 11:1439–1447. [PubMed: 12023986]

Collins CA, Olsen I, Zammit PS, Heslop L, Petrie A, Partridge TA, Morgan JE. Stem cell function, self-renewal, and behavioral heterogeneity of cells from the adult muscle satellite cell niche. Cell. 2005; 122:289–301. [PubMed: 16051152]

Conboy IM, Conboy MJ, Smythe GM, Rando TA. Notch-mediated restoration of regenerative potential to aged muscle. Science. 2003; 302:1575–1577. [PubMed: 14645852]

Coovert DD, Le TT, McAndrew PE, Strasswimmer J, Crawford TO, Mendell JR, Coulson SE, Androphy EJ, Prior TW, Burghes AH. The survival motor neuron protein in spinal muscular atrophy. Hum. Mol. Genet. 1997; 6:1205–1214. [PubMed: 9259265]

Cornelison DD, Filla MS, Stanley HM, Rapraeger AC, Olwin BB. Syndecan-3 and syndecan-4 specifically mark skeletal muscle satellite cells and are implicated in satellite cell maintenance and muscle regeneration. Dev. Biol. 2001; 239:79–94. [PubMed: 11784020]

Crawford TO, Pardo CA. The neurobiology of childhood spinal muscular atrophy. Neurobiol. Dis. 1996; 3:97–110. [PubMed: 9173917]

DiDonato CJ, Chen XN, Noya D, Korenberg JR, Nadeau JH, Simard LR. Cloning, characterization, and copy number of the murine survival motor neuron gene: homolog of the spinal muscular atrophy-determining gene. Genome Res. 1997; 7:339–352. [PubMed: 9110173]

Feldkotter M, Schwarzer V, Wirth R, Wienker TF, Wirth B. Quantitative analyses of SMN1 and SMN2 based on real-time lightCycler PCR: fast and highly reliable carrier testing and prediction of severity of spinal muscular atrophy. Am. J. Hum. Genet. 2002; 70:358–368. [PubMed: 11791208]

Gavrilina TO, McGovern VL, Workman E, Crawford TO, Gogliotti RG, DiDonato CJ, Monani UR, Morris GE, Burghes AH. Neuronal SMN expression corrects spinal muscular atrophy in severe SMA mice while muscle-specific SMN expression has no phenotypic effect. Hum. Mol. Genet. 2008; 17:1063–1075. [PubMed: 18178576]

Gavrilov DK, Shi X, Das K, Gilliam TC, Wang CH. Differential SMN2 expression associated with SMA severity. Nat Genet. 1998; 20:230–231. [PubMed: 9806538]

Guettier-Sigrist S, Hugel B, Coupin G, Freyssinet JM, Poindron P, Warter JM. Possible pathogenic role of muscle cell dysfunction in motor neuron death in spinal muscular atrophy. Muscle Nerve. 2002; 25:700–708. [PubMed: 11994964]

Hawke TJ, Garry DJ. Myogenic satellite cells: physiology to molecular biology. J. Appl. Physiol. 2001; 91:534–551. [PubMed: 11457764]

NIH-PA Author Manuscript NIH-PA Author Manuscript NIH-PA Author Manuscript

Henderson CE, Hauser SL, Huchet M, Dessi F, Hentati F, Taguchi T, Changeux JP, Fardeau M. Extracts of muscle biopsies from patients with spinal muscular atrophies inhibit neurite outgrowth from spinal neurons. Neurology. 1987; 37:1361–1364. [PubMed: 3614658]

Joe AW, Yi L, Natarajan A, Le Grand F, So L, Wang J, Rudnicki MA, Rossi FM. Muscle injury activates resident fibro/adipogenic progenitors that facilitate myogenesis. Nat. Cell Biol. 2010; 12:153–163. [PubMed: 20081841]

Kariya S, Park GH, Maeno-Hikichi Y, Leykekhman O, Lutz C, Arkovitz MS, Landmesser LT, Monani UR. Reduced SMN protein impairs maturation of the neuromuscular junctions in mouse models of spinal muscular atrophy. Hum. Mol. Genet. 2008; 17:2552–2569. [PubMed: 18492800]

Kuang S, Kuroda K, Le Grand F, Rudnicki MA. Asymmetric self-renewal and commitment of satellite stem cells in muscle. Cell. 2007; 129:999–1010. [PubMed: 17540178]

Le TT, Pham LT, Butchbach ME, Zhang HL, Monani UR, Coovert DD, Gavrilina TO, Xing L, Bassell GJ, Burghes AH. SMNDelta7, the major product of the centromeric survival motor neuron (SMN2) gene, extends survival in mice with spinal muscular atrophy and associates with full-length SMN. Hum. Mol. Genet. 2005; 14:845–857. [PubMed: 15703193]

Lee YI, Mikesh M, Smith I, Rimer M, Thompson W. Muscles in a mouse model of spinal muscular atrophy show profound defects in neuromuscular development even in the absence of failure in neuromuscular transmission or loss of motor neurons. Dev. Biol. 2011

Lefebvre S, Burglen L, Reboullet S, Clermont O, Burlet P, Viollet L, Benichou B, Cruaud C, Millasseau P, Zeviani M, et al. Identification and characterization of a spinal muscular atrophy-determining gene. Cell. 1995; 80:155–165. [PubMed: 7813012]

Lorson CL, Hahnen E, Androphy EJ, Wirth B. A single nucleotide in the SMN gene regulates splicing and is responsible for spinal muscular atrophy. Proc. Natl. Acad. Sci. U S A. 1999; 96:6307–6311. [PubMed: 10339583]

McGovern VL, Gavrilina TO, Beattie CE, Burghes AH. Embryonic motor axon development in the severe SMA mouse. Hum. Mol. Genet. 2008; 17:2900–2909. [PubMed: 18603534]

McWhorter ML, Monani UR, Burghes AH, Beattie CE. Knockdown of the survival motor neuron (Smn) protein in zebrafish causes defects in motor axon outgrowth and pathfinding. J. Cell Biol. 2003; 162:919–931. [PubMed: 12952942]

Monani UR, Sendtner M, Coovert DD, Parsons DW, Andreassi C, Le TT, Jablonka S, Schrank B, Rossoll W, Prior TW, et al. The human centromeric survival motor neuron gene (SMN2) rescues embryonic lethality in Smn(−/−) mice and results in a mouse with spinal muscular atrophy. Hum. Mol. Genet. 2000; 9:333–339. [PubMed: 10655541]

Montarras D, Morgan J, Collins C, Relaix F, Zaffran S, Cumano A, Partridge T, Buckingham M. Direct isolation of satellite cells for skeletal muscle regeneration. Science. 2005; 309:2064–2067. [PubMed: 16141372]

Murray LM, Comley LH, Thomson D, Parkinson N, Talbot K, Gillingwater TH. Selective vulnerability of motor neurons and dissociation of pre-and post-synaptic pathology at the neuromuscular junction in mouse models of spinal muscular atrophy. Hum. Mol. Genet. 2008; 17:949–962. [PubMed: 18065780]

Nicole S, Desforges B, Millet G, Lesbordes J, Cifuentes-Diaz C, Vertes D, Cao ML, De Backer F, Languille L, Roblot N, et al. Intact satellite cells lead to remarkable protection against Smn gene defect in differentiated skeletal muscle. J. Cell Biol. 2003; 161:571–582. [PubMed: 12743106]

Park GH, Kariya S, Monani UR. Spinal muscular atrophy: new and emerging insights from model mice. Curr. Neurol. Neurosci. Rep. 2010; 10:108–117. [PubMed: 20425235]

Rajendra TK, Gonsalvez GB, Walker MP, Shpargel KB, Salz HK, Matera AG. A Drosophila melanogaster model of spinal muscular atrophy reveals a function for SMN in striated muscle. J. Cell Biol. 2007; 176:831–841. [PubMed: 17353360]

Rossoll W, Jablonka S, Andreassi C, Kroning AK, Karle K, Monani UR, Sendtner M. Smn, the spinal muscular atrophy-determining gene product, modulates axon growth and localization of beta-actin mRNA in growth cones of motoneurons. J. Cell. Biol. 2003; 163:801–812. [PubMed: 14623865]

Schulz TJ, Huang TL, Tran TT, Zhang H, Townsend KL, Shadrach JL, Cerletti M, McDougall LE, Giorgadze N, Tchkonia T, et al. Identification of inducible brown adipocyte progenitors residing in

NIH-PA Author Manuscript

NIH-PA Author Manuscript

NIH-PA Author Manuscript

skeletal muscle and white fat. Proc. Natl. Acad. Sci. U S A. 2011; 108:143–148. [PubMed: 21173238]

Seale P, Sabourin LA, Girgis-Gabardo A, Mansouri A, Grass P, Rudnicki MA. Pax7 is required for the specification of myogenic satellite cells. Cell. 2000; 102:777–786. [PubMed: 11030621]

Shafey D, Cote PD, Kothary R. Hypomorphic Smn knockdown C2C12 myoblasts reveal intrinsic defects in myoblast fusion and myotube morphology. Exp. Cell Res. 2005; 311:49–61. [PubMed: 16219305]

Shafey D, MacKenzie AE, Kothary R. Neurodevelopmental abnormalities in neurosphere-derived neural stem cells from SMN-depleted mice. J. Neurosci. Res. 2008; 86:2839–2847. [PubMed: 18521935]

Sherwood RI, Christensen JL, Conboy IM, Conboy MJ, Rando TA, Weissman IL, Wagers AJ. Isolation of adult mouse myogenic progenitors: functional heterogeneity of cells within and engrafting skeletal muscle. Cell. 2004; 119:543–554. [PubMed: 15537543]

Uezumi A, Fukada S, Yamamoto N, Takeda S, Tsuchida K. Mesenchymal progenitors distinct from satellite cells contribute to ectopic fat cell formation in skeletal muscle. Nat. Cell Biol. 2010; 12:143–152. [PubMed: 20081842]

Venuti JM, Morris JH, Vivian JL, Olson EN, Klein WH. Myogenin is required for late but not early aspects of myogenesis during mouse development. J. Cell Biol. 1995; 128:563–576. [PubMed: 7532173]

Wagers AJ, Conboy IM. Cellular and molecular signatures of muscle regeneration: current concepts and controversies in adult myogenesis. Cell. 2005; 122:659–667. [PubMed: 16143100]

Zammit PS. All muscle satellite cells are equal, but are some more equal than others? J. Cell Sci. 2008; 121:2975–2982. [PubMed: 18768931]

NIH-PA Author Manuscript

NIH-PA Author Manuscript

NIH-PA Author Manuscript

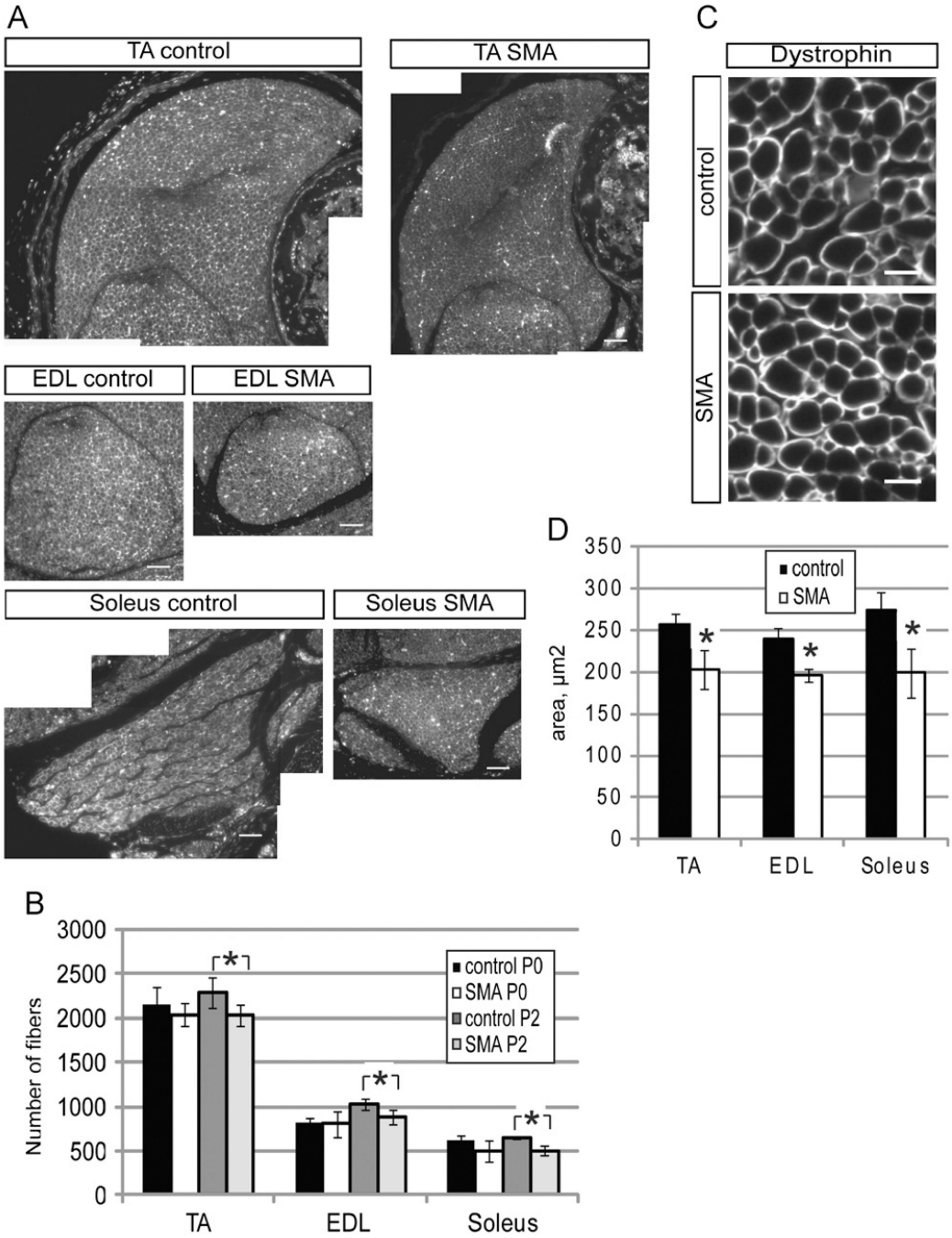

Fig. 1. Smn deficient animals have fewer and smaller myofibers

(A) Individual TA, EDL, and soleus muscles from control and SMA mice were stained with an anti-dystrophin antibody to visualize individual muscle fibers. (B) Quantitation of fiber number in the TA, EDL, and soleus muscles revealed that SMA mice have significantly fewer fibers in all muscle groups at P2, but not at P0. (C) Higher magnification micrograph of muscle cross sections after dystrophin staining. Scalebar 10 uM. (D) The average area per muscle fiber was significantly reduced in TA, EDL, and soleus muscles. $^{*}P < 0.05$, paired *t*-test. Data are presented as mean ± s.d.

NIH-PA Author Manuscript

NIH-PA Author Manuscript

NIH-PA Author Manuscript

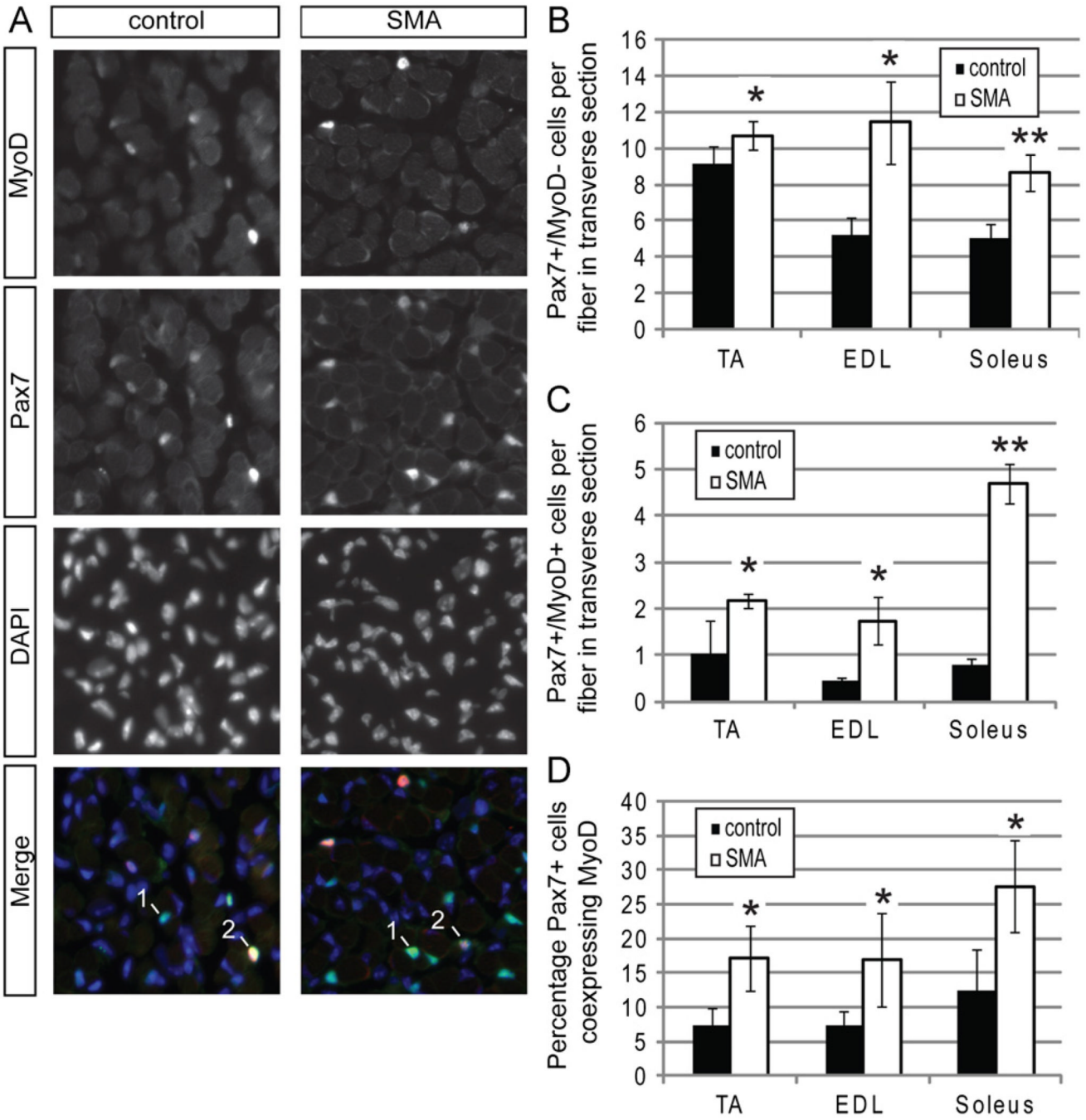

Fig. 2. Smn deficient satellite cells differentiate prematurely in vivo

Sections from 3 muscles of P2 mice were co-stained with anti-Pax7 and anti-MyoD antibodies. (A) Representative images from the EDL muscle showing staining for Pax7 (green in merged image) MyoD (red in merged image) and DAPI (blue in merged image). We classified cells as $Pax7^{+}/MyoD^{-}$ satellite cells (labeled 1) or $Pax7^{+}MyoD^{+}$ myogenic progenitors (labeled 2) and quantified them in comparable transverse sections of all three muscle groups. (B) There is a large number of $Pax7^{+}/MyoD^{-}$ cells per fiber in all SMA muscle groups. (C) All SMA muscle groups had significantly higher numbers of $Pax7^{+}/MyoD^{+}$ cells per fiber. (D)The percentage of $Pax7^{+}$ cells that are also $MyoD^{+}$ is also

elevated in SMA muscle. $^{*}P < 0.05$, paired *t*-test. $^{**}P < 0.005$, paired *t*-test. Data are presented as mean ± s.d. (For interpretation of the references to color in this figure legend, the reader is referred to the web version of this article.)

NIH-PA Author Manuscript
NIH-PA Author Manuscript
NIH-PA Author Manuscript

NIH-PA Author Manuscript

NIH-PA Author Manuscript

NIH-PA Author Manuscript

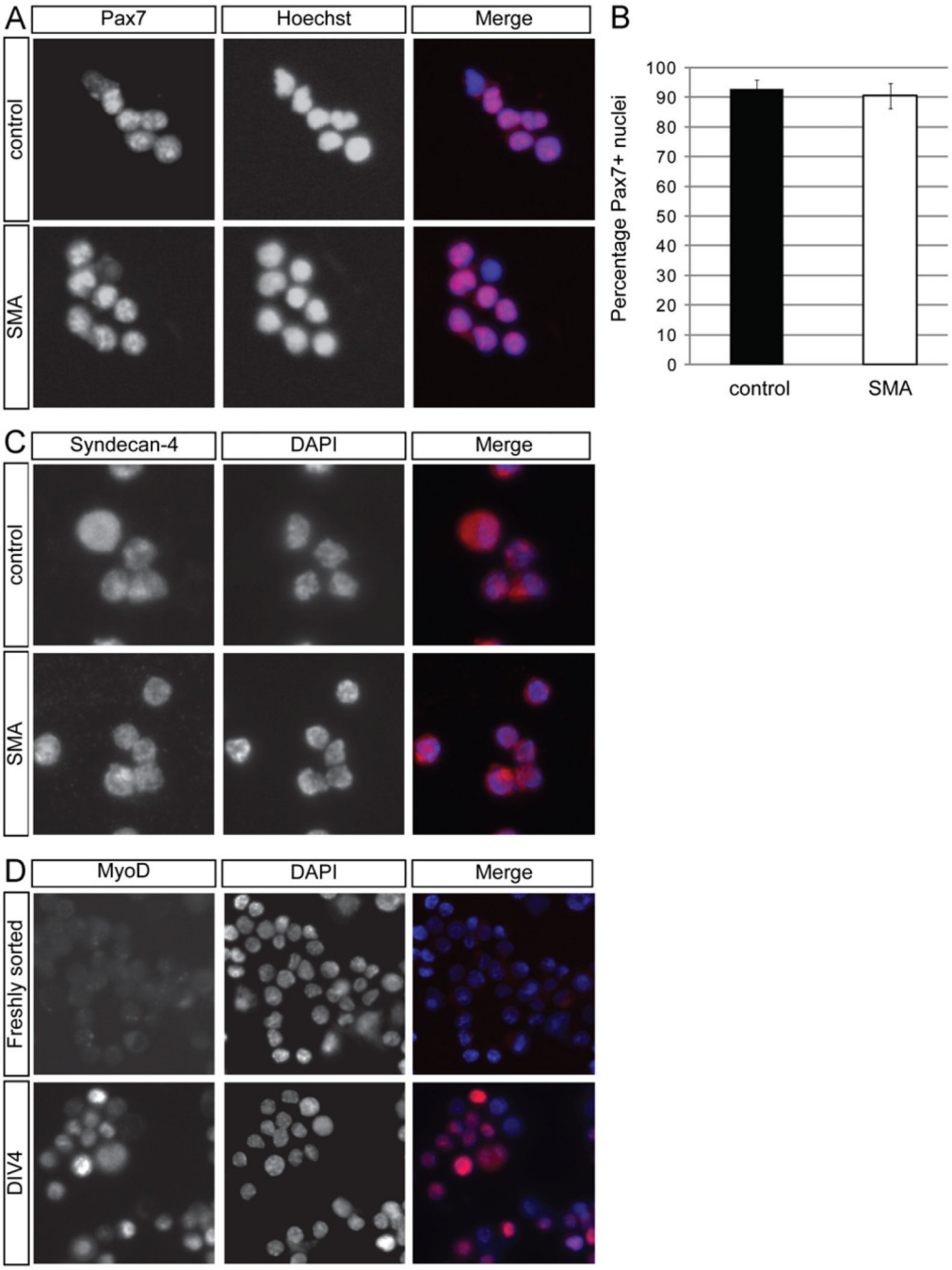

Fig. 3. Freshly sorted satellite cells express the satellite cell markers Pax7 and Syndecan −4

(A) Pax7 immunostaining (red in merged image) was performed on freshly isolated satellite cells from P2 control and SMA muscle. Nuclei were labeled with DAPI (blue in merged image). (B) Quantitation of the percentage of $Pax7^{+}$ nuclei from freshly sorted satellite cells. Data are presented as mean ± s.d. All freshly sorted cells from both types of P2 muscle were Syndecan-4 positive (C; red in merged image) and MyoD negative (D; red in merged image). (D) Freshly sorted satellite cells were MyoD negative, but after four days (DIV4) in culture, cells began to express MyoD. Nuclei were marked with DAPI (blue in merged image). (For interpretation of the references to color in this figure legend, the reader is referred to the web version of this article.)

NIH-PA Author Manuscript

NIH-PA Author Manuscript

NIH-PA Author Manuscript

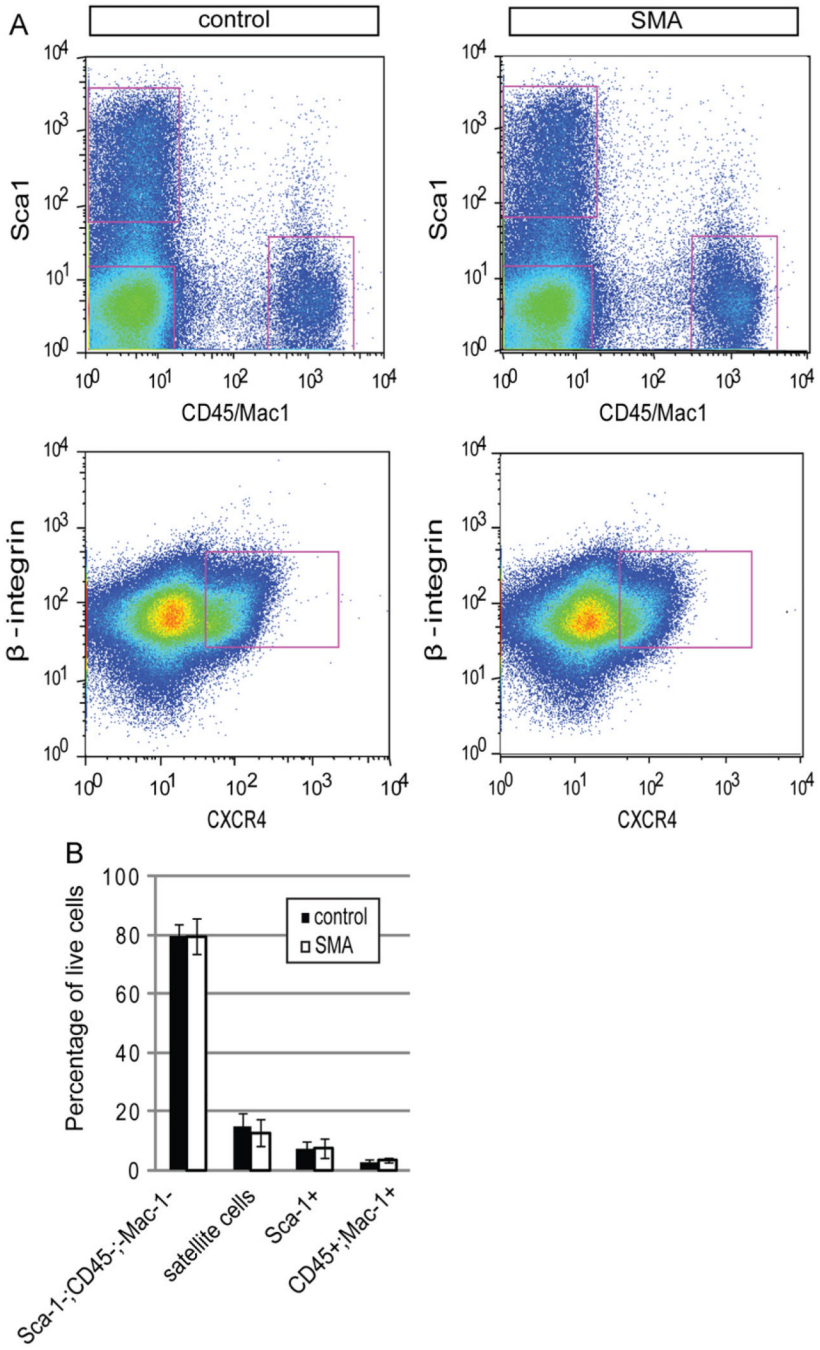

Fig. 4. Normal frequencies of myofiber-associated cells isolated from SMA mice

(A) Representative plots showing FACS analyses of myofiber-associated cells from P2 control and SMA muscle. (B) Quantification of the percentage of each subpopulation with respect to the total viable population (calcein positive and propidium iodide negative). The frequencies of Sca-1^{-};CD45^{-};Mac-1^{-} cells, satellite cells (CXCR4^{+};β-integrin^{+}), fibroblasts and adipogenic precursor cells (Sca-1^{+}), and hematopoietic cells (CD45 $^{+}$;Mac-1^{+}) were comparable between control and SMA muscle. Data are presented as mean ± s.d.

NIH-PA Author Manuscript

NIH-PA Author Manuscript

NIH-PA Author Manuscript

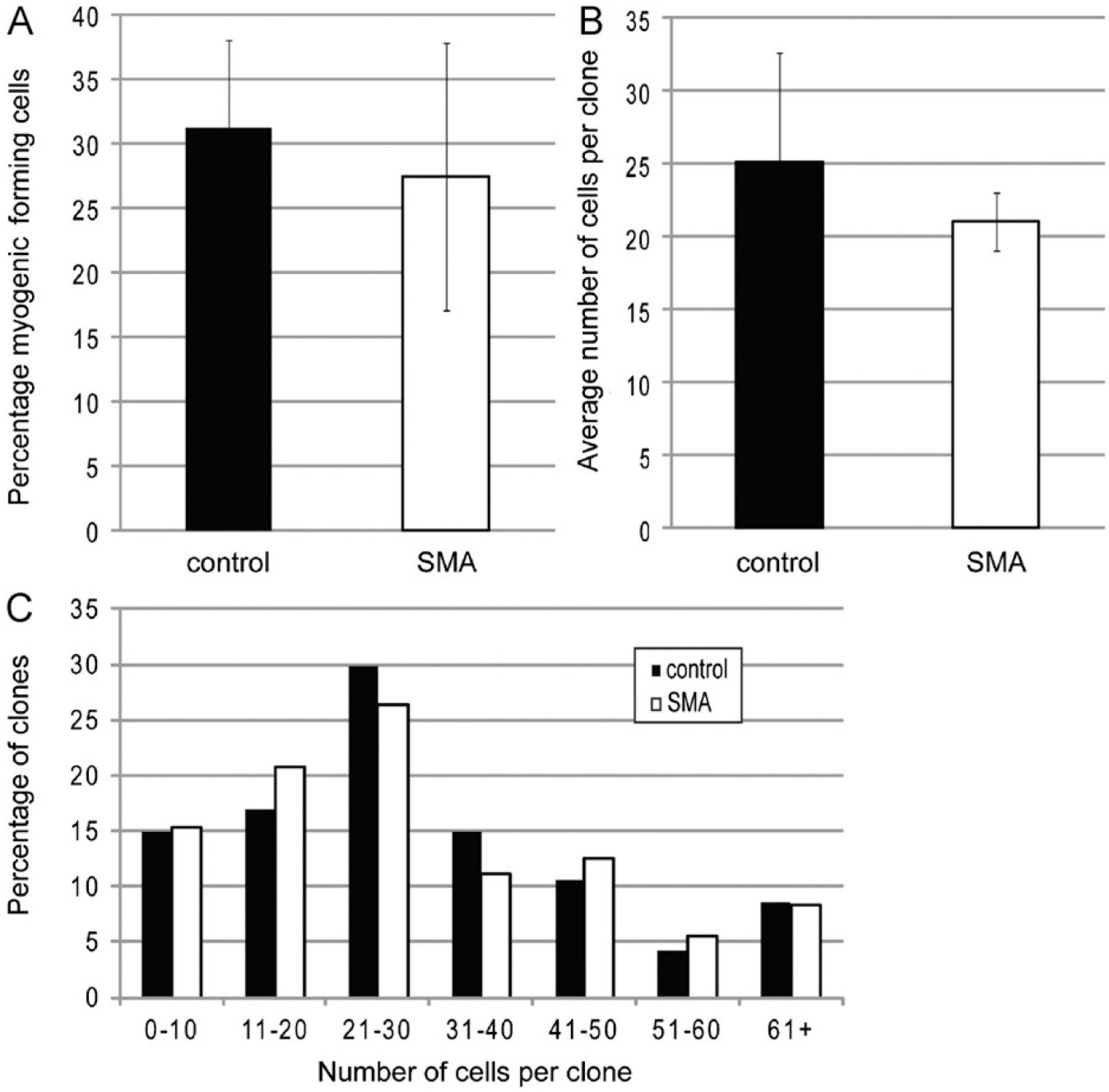

Fig. 5. Sorted satellite cells have normal survival and proliferation

(A) Quantitation of the efficiency of colony formation of sorted cells. (B) Quantification of the number of cells per clone. Data are presented as mean ± s.d. (C) Percentage of clones with indicated number of cells per clone. All measurements were made on DIV4.

NIH-PA Author Manuscript

NIH-PA Author Manuscript

NIH-PA Author Manuscript

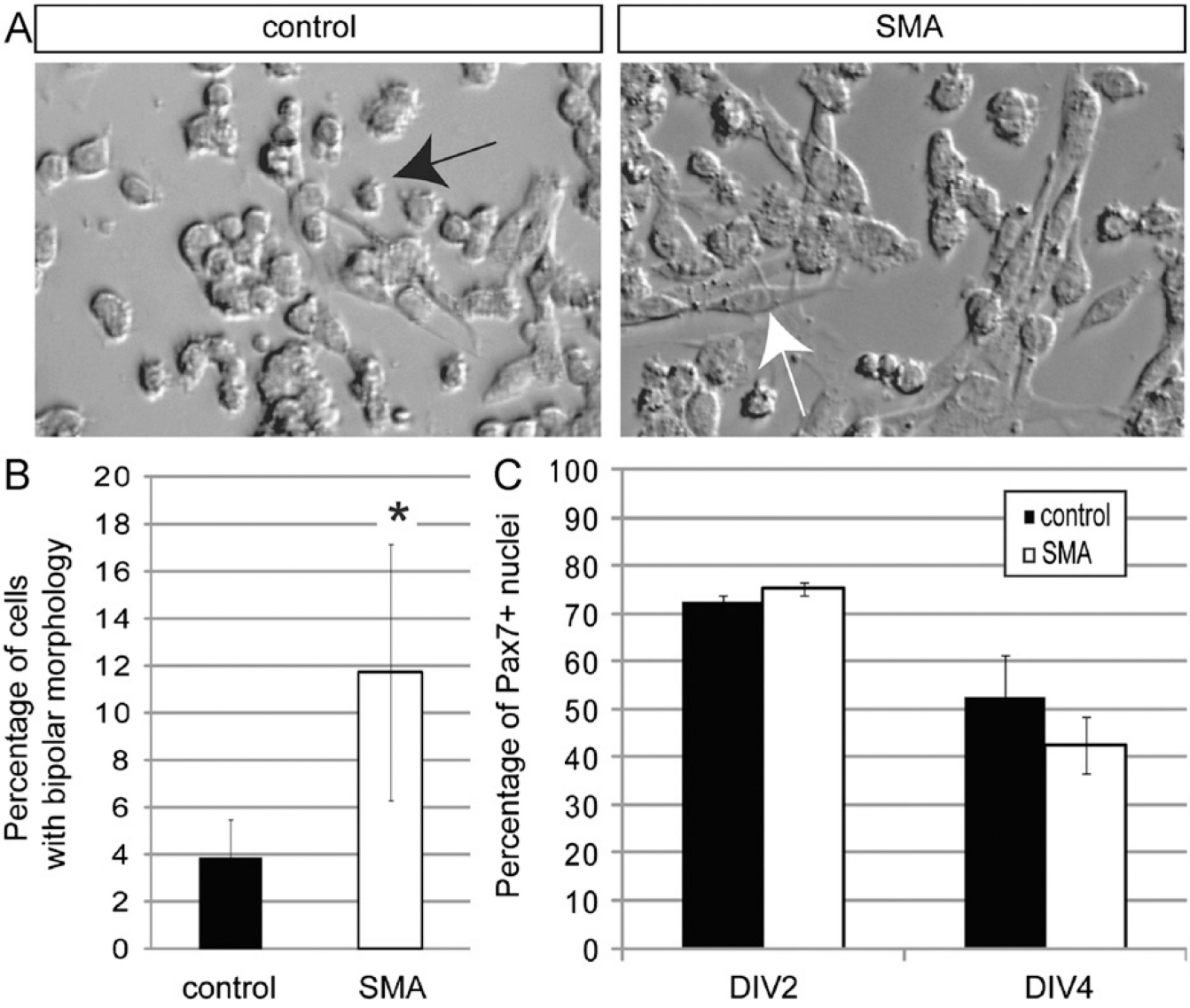

Fig. 6. SMN deficient satellite cells prematurely exhibit a bipolar, myoblast morphology

(A) Brightfield images of satellite cell derived cultures on DIV4. Cells appear to adopt either a round or bipolar morphology. Round cells are marked with a black arrow; bipolar, myoblast-like cells are marked with a white arrow. (B) The frequency of cells with a myoblast-like morphology was higher in SMA muscle cultures on DIV4. (C) Cultures were stained on DIV2 and DIV4 with an anti-Pax7 antibody to quantify the frequency of satellite cells remaining in the cultures. The percentage of Pax7 positive nuclei was comparable in the two different types of cultures on both days. $^{*}P < 0.005$, paired *t*-test. Data presented as mean ± s.d.

NIH-PA Author Manuscript

NIH-PA Author Manuscript

NIH-PA Author Manuscript

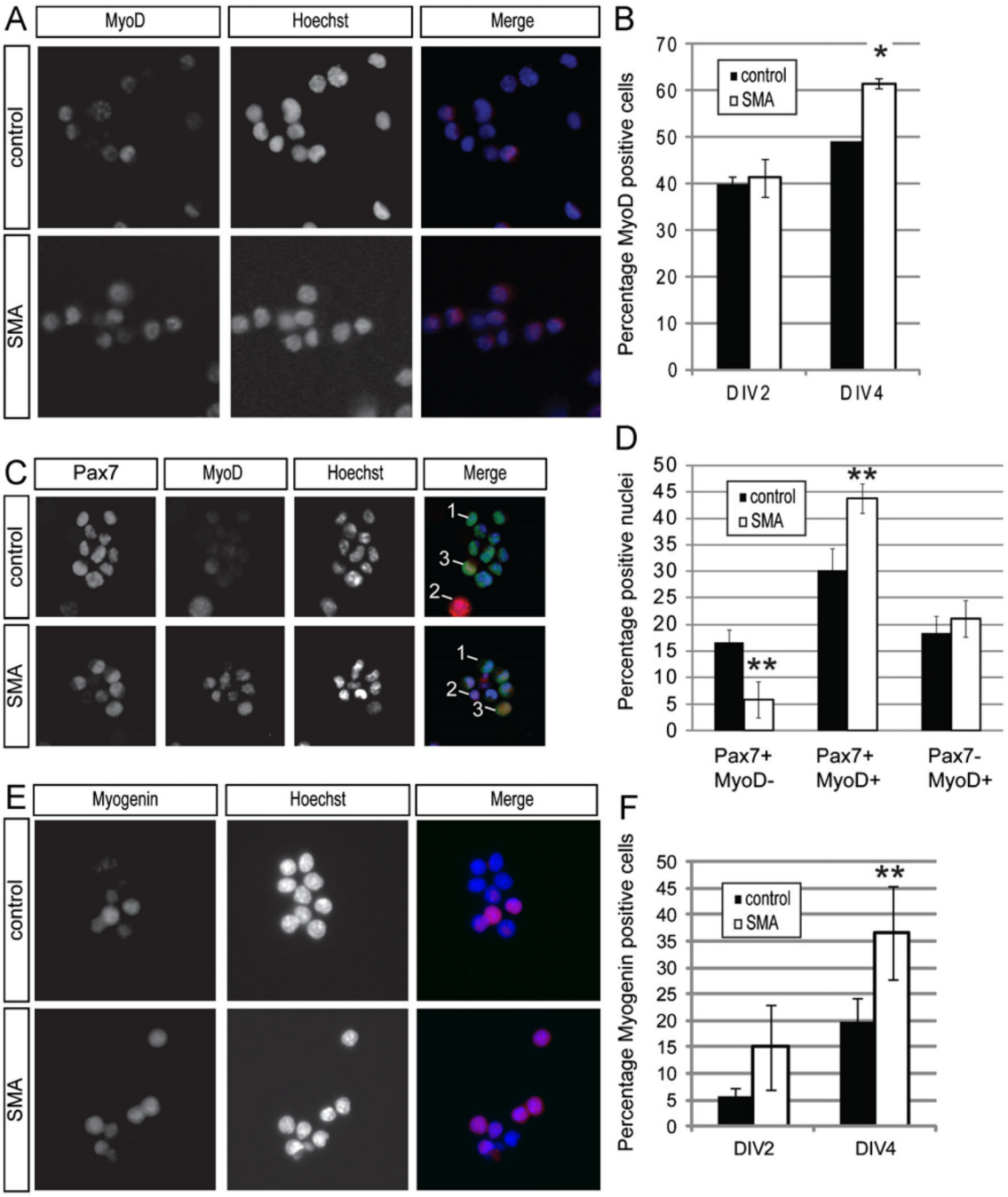

Fig. 7. SMN deficient cells express myogenic markers more quickly

(A) Representative images of DIV4 cultured cells stained for MyoD expression (red in merged image). Nuclei are marked by DAPI (blue in merged image). (B) A greater percentage of cells are $MyoD^+$ in SMA cultures on DIV4, but not on DIV2. (C) Co-staining with anti-Pax7 and anti-MyoD antibodies in DIV4 cultures reveals cells that: express Pax7 only (1, green in merged image), MyoD only (2, red in merged image), or both Pax7 and MyoD. Nuclei are marked by DAPI (blue in merged image). (D) DIV4 SMA muscle cultures have fewer $Pax7^+/MyoD^-$ cells, but a higher frequency of $Pax7^+/MyoD^+$ cells. The percentage of $Pax7^-/MyoD^+$ cells is similar in the two cultures. (E) Representative images of DIV4 cultured cells stained for myogenin (red in merged image). Nuclei are marked by

NIH-PA Author Manuscript

NIH-PA Author Manuscript

NIH-PA Author Manuscript

Hoechst (blue in merged image). (F) SMA muscle cultures have a higher percentage of myogenin positive cells at DIV4. $^{*}P < 0.05$, paired *t*-test. $^{**}P < 0.005$, paired *t*-test. Data presented as mean ± s.d. (For interpretation of the references to color in this figure legend, the reader is referred to the web version of this article.)

NIH-PA Author Manuscript

NIH-PA Author Manuscript

NIH-PA Author Manuscript

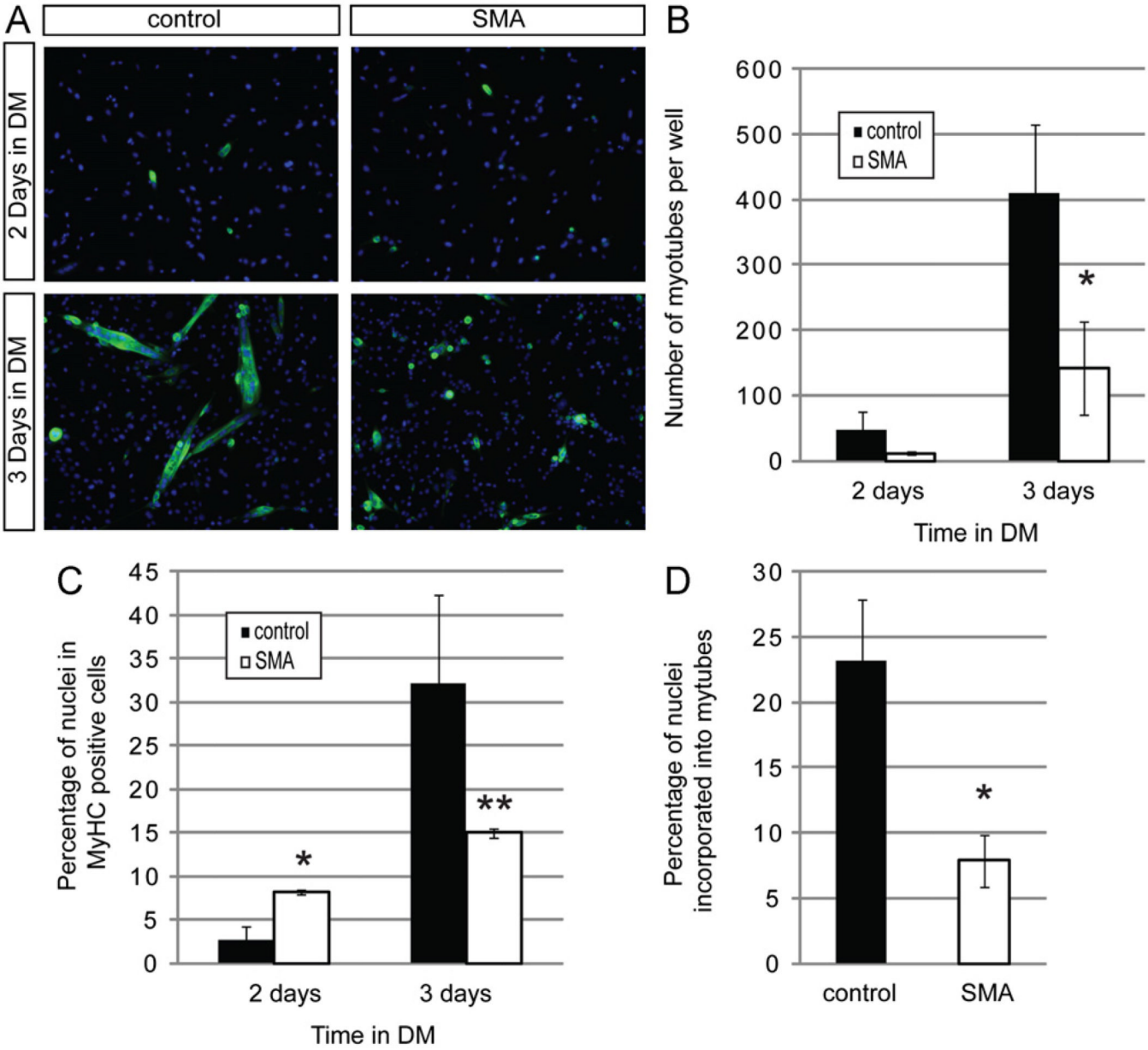

Fig. 8. SMN deficient satellite cells grown under differentiation conditions form fewer myotubes

(A) Representative images showing staining of MyHC^{+} cells (green) in cultures grown in differentiation media (DM) for 2 and 3 days. Nuclei are marked with Hoechst (blue). (B) Myotubes were defined as cells containing 2 or more nuclei in a MyHC positive cytoplasm. After 3 days in DM, control cells form significantly more myotubes than SMA cells. (C) The frequency of MyHC positive cells is elevated in SMN deficient cultures 2 days after treatment with DM but is reduced after 3 days in DM when cells fail to form myotubes efficiently. (D) There is also a reduction in myotube formation in the SMA cultures when measured as the percentage of nuclei found in myotubes. $^{*}P < 0.05$, paired *t*-test. $^{**}P < 0.005$, paired *t*-test. Data represent mean ± s.d. (For interpretation of the references to color in this figure legend, the reader is referred to the web version of this article.)